Global and Planetary Change 156 (2017) 1–12

Contents lists available at ScienceDirect

Global and Planetary Change

journal homepage: www.elsevier.com/locate/gloplacha

# Hydro-thermal processes and thermal offsets of peat soils in the active layer in an alpine permafrost region, NE Qinghai-Tibet plateau

Qingfeng Wang[a], Huijun Jin[a,b,*], Tingjun Zhang[c,**], Bin Cao[c], Xiaoqing Peng[c], Kang Wang[d], Xiongxin Xiao[c], Hong Guo[c], Cuicui Mu[c], Lili Li[c]

[a] State Key Laboratory of Frozen Soil Engineering, Northwest Institute of Eco-Environment and Resources, 4, 320 West Donggang Road, Lanzhou 730000, China
[b] School of Civil Engineering, Harbin Institute of Technology, 73 Huanghe Road, Harbin 150090, China
[c] Key Laboratory of Western China's Environmental Systems (Ministry of Education),College of Earth and Environmental Sciences, Lanzhou University, 222 South Tianshui Road, Lanzhou 730000, China
[d] Institute of Arctic and Alpine Research, University of Colorado at Boulder, Boulder, CO 80309-0545, USA

## ARTICLE INFO

*Keywords:*
Lower limit of permafrost (LLP)
Active layer processes
Peatlands
Permafrost degradation
Upper Heihe River Basin (UHRB)

## ABSTRACT

Observation data of the hydrothermal processes in the active layer are vital for the verification of permafrost formation and evolution, eco-hydrology, ground-atmosphere interactions, and climate models at various time and spatial scales. Based on measurements of ground temperatures in boreholes, of temperatures and moisture contents of soils in the active layer, and of the mean annual air temperatures at the Qilian, Yeniugou and Tuole meteorological stations in the upper Heihe River Basin (UHRB) and the adjacent areas, a series of observations were made concerning changes in the lower limit of permafrost (LLP) and the related hydrothermal dynamics of soils in the active layer. Because of the thermal diode effect of peat soils, the LLP (at 3600 m) was lower on the northern slope of the Eboling Mountains at the eastern branch of the UHRB than that (at 3650–3700 m) on the alluvial plain at the western branch of the UHRB. The mean temperature of soils at depths of 5 to 77 cm in the active layer on peatlands was higher during periods with subzero temperatures and lower during periods with above-zero temperatures in the vicinity of the LLP on the northern slope of the Eboling Mountains than those at the LLP at the western branch of the UHRB. The thawing and downward freezing rates of soils in the active layer near the LLP on the northern slope of the Eboling Mountains were 0.2 and 1.6 times those found at the LLP at the western branch of the UHRB. From early May to late August, the soil water contents at the depths of 20 to 60 cm in the active layer near the LLP on the northern slope of the Eboling Mountains were significantly lower than those found at the LLP at the western branch of the UHRB. The annual ranges of soil temperatures (ARSTs), mean annual soil temperatures (MASTs) in the active layer on peatlands, and the mean annual ground temperature (MAGT) at a depth of 14 m of the underlying permafrost were all significantly lower near the LLP on the northern slope of the Eboling Mountains. Moreover, the thermophysical properties of peat soils and high moisture contents in the active layer on peatlands resulted in the lower soil temperatures in the active layer close to the LLP on the northern slope of the Eboling Mountains than those found at the LLP at the western branch of the UHRB in the warm season, especially at the deeper depths (20–77 cm). They also resulted in the smaller freezing index (FI) and thawing index (TI) and larger FI/TI ratios of soils at the depths of 5 to 77 cm in the active layer near the LLP on the northern slope of the Eboling Mountains. In short, peatlands have unique thermophysical properties for reducing heat absorption in the warm season and for limiting heat release in the cold season as well. However, the permafrost zone has shrunk by 10–20 km along the major highways at the western branch of the UHRB since 1985, and a medium-scale retrogressive slump has occurred on the peatlands on the northern slope of the Eboling Mountains in recent decades. The results can provide basic data for further studies of the hydrological functions of different landscapes in alpine permafrost regions. Such studies can also enable evaluations and forecasts the hydrological impacts of changing frozen ground in the UHRB and of other alpine mountain regions in West China.

* Correspondence to: H. Jin, State Key Laboratory of Frozen Soil Engineering, Northwest Institute of Eco-Environment and Resources, Chinese Academy of Sciences, 320 West Donggang Road, Lanzhou 730000, China.
** Corresponding author.
*E-mail addresses:* hjjin@lzb.ac.cn (H. Jin), tjzhang@lzu.edu.cn (T. Zhang).

http://dx.doi.org/10.1016/j.gloplacha.2017.07.011
Received 20 November 2016; Received in revised form 3 June 2017; Accepted 15 July 2017
Available online 17 July 2017

## 1. Introduction

Many rivers originate from the cold regions in West China. Thus, as the "water towers", they provide the main water sources for the semi-arid and arid areas. In the context of climate warming and drying, cold regions hydrology has become a major research focus recently (e.g., Peterson et al., 2002; Ding and Xiao, 2013). Studies on the hydrological functions of different landscapes in cold regions provide an important scientific basis for the planning and utilization of regional water resources and environmental restoration (Wang et al., 2009a; Chen et al., 2014). However, relevant studies are very limited so far, those in permafrost regions in particular.

In recent decades, changes in the distribution of permafrost and taliks and in the seasonal freeze-thaw cycles have dramatically changed the hydrology and hydrogeology in cold regions (e.g., Serreze et al., 2000; Carey and Woo, 2001; Yang et al., 2004a; ACIA, 2005; Hinzman et al., 2005; Jorgenson et al., 2006; Gruber and Haeberli, 2009; Cheng and Jin, 2013; Zhang et al., 2013a). These changes in permafrost and freeze-thaw regimes have important effects on the runoff generation and peak flows, on the annual and interannual variations in flow processes, and on the dynamics for the recharge, flowpaths and discharge of groundwater.

Frozen ground hydrology is key in linking the eco-hydrological processes of cold regions (e.g., Cheng and Zhou, 1988; Woo et al., 2008; Cheng and Jin, 2013). Observational data of the hydrothermal processes in the active layer are vital for the verification of permafrost formation and evolution, eco-hydrology, ground-atmosphere interactions, and climate models at various time and spatial scales (e.g., Saito et al., 2007). The degradation of frozen ground, as induced by climate change and human activities, has resulted in ground warming and deepening active layer, rising of the lower limit of permafrost (LLP) (e.g., Jin et al., 2000, 2006; Cheng and Wu, 2007; Zhao et al., 2010; Wu et al., 2015) and reduction in the maximum depths of seasonal frost penetration (Wang et al., 2015a; Qin et al., 2016). Such degradation has significantly changed the eco-hydrogeological environment in cold regions, and will certainly have important impacts on the hydrological processes and water resources dynamics in the headwaters of major rivers in the future. These effects will include the lowering of the superpermafrost water table, increases in the thickness of vadose zones (Cao et al., 2003), shifts in aquifer permeability and water-holding capacity (Bense et al., 2009, 2012), enhanced infiltration of precipitation and groundwater recharge to base flows (Qin et al., 2016; Gao et al., 2016), slight enhancements of surface hydrological processes (Lan et al., 2015), changes in spring vegetation green-up dates (Piao et al., 2011; Zhang et al., 2013b; Qin et al., 2016), and the overall degradation of alpine ecosystems (e.g., Jorgenson et al., 2001; Zhao and Zhou, 2005; Wang et al., 2006; Yi et al., 2011, 2014; Wang et al., 2016a). Therefore, questions concerning the processes and mechanisms by which permafrost responds to climate change over different spatial and temporal scales, and the influences of thawing ground ice on hydrological cycles and water resources, are pressing issues in the field of cold regions hydrology (Cheng and Jin, 2013).

In the upper Heihe River Basin (UHRB) of the Qilian Mountains on NE Qinghai-Tibet Plateau (QTP), the alpine cryosphere above 3600 m a.s.l. is the main runoff-generation area, which produces > 80% of the river runoff (Kang et al., 2008; Wang et al., 2009a). From 1960 to 2013, the volumes of runoff in the UHRB were on the rise, and mainly due to the increased base flow (Qin et al., 2016). Moreover, the recession coefficients of runoff at the Yingluoxia Hydrological Station (at the piedmont of the UHRB) showed a significant spike over the previous 50 years (Niu et al., 2011).

Similar trends were also found in the Lena, Yenisei and Ob river basins in Siberia (e.g., Peterson et al., 2002; Ye et al., 2003; Yang et al., 2004a, 2004b; Zhang et al., 2005). Qin et al. (2016) proposed that the increases in precipitation and the decreases in maximum depths of seasonal frost penetration were the major contributors for the increased base flow. It has been presumed that this increase in base flow may be due to rising precipitation and to increased infiltration and storage capacity of the active layer soils, as a result of the deepening active layer thickness under a warming climate (e.g., Serreze et al., 2000; Zhang et al., 2005; Ye et al., 2009; Niu et al., 2011; Zhang et al., 2013a; Wang et al., 2015b; Qin et al., 2016).

Recently, observations and simulations have been carried out in the Binggou sub-basin of the UHRB on the freeze-thaw processes, stream flows, and the effects of snow cover and organic matter on these hydrological processes (Zhang et al., 2013c; Zhou et al., 2013, 2014). In the Hulugou sub-basin, the hydrothermal processes in the active layer in alpine cold desert and paludal alpine meadow were observed and simulated, and the alpine cold desert zone was identified as the main runoff generation area in the UHRB (Yang et al., 2013; Chen et al., 2014). A number of reports have been published on the characteristics of permafrost (Wang et al., 2013), the freeze-thaw process of soils in the active layer (Yang et al., 2013; Wang et al., 2016b; Cao et al., 2017), the effects that snow cover and organic matter have on active layer freeze-thaw processes and stream flow regimes (Zhang et al., 2013c; Zhou et al., 2013, 2014), the hydrological functions of several representative underlying surfaces (Chen et al., 2014), and the contribution of ground-ice meltwater to stream-flows (Li et al., 2014, 2016). Other studies have examined the physical and chemical properties of soils, and the effects of these properties on the carbon and nitrogen dynamics of soils in the active layer and shallow permafrost (Mu et al., 2015, 2016). However, the conditions and changes in the LLP, and the hydrothermal processes of soils in the active layer at the LLP, remain unclear in regard to the UHRB.

The aims of this study are as follows: (1) to clearly identify the LLP at the eastern and western branches of the UHRB, and to discuss the possible eco-hydrological impacts of permafrost degradation; (2) to explore changes in the hydrothermal dynamics of soils in the active layer in the vicinity of the LLP, and to determine how these dynamics influence the elevations of the LLP. The results of this study can provide basic data for further studies on the hydrological functions of different landscapes in alpine permafrost regions, and for evaluation or forecasts concerning the hydrological impacts of frozen ground degradation in the UHRB and in other alpine mountains in West China.

## 2. Study area and data

### 2.1. Study area

The Heihe River Basin is located on the northern flank of the Qilian Mountains, on the northeastern margin of the QTP. This basin has a main stream length of ~819 km and a drainage area of 1,432,000 km$^2$ (Li et al., 2013). The area ranges between 97.1°–102.0°E (eastern longitudes) and 37.7°–42.7°N (northern latitudes). The UHRB, with an elevation ranging between 1600 m and 5400 m a.s.l., has a (sub-)alpine semi-arid climate. The mean annual air temperature (MAAT) is lower than 2 °C, and the annual precipitation ranges from 200 mm to 700 mm, increasing eastwards and with elevation.

The vegetation is characteristic of temperate mountain forest steppes and meadows, with a scattered but widespread presence of shrublands and forests. The vertical zonation of soil and vegetation is evident. Under the constraints of hydrothermal conditions closely related to elevation and slope, the soils can be divided into three major types, i.e., the alpine, subalpine and piedmont hilly soil types. The alpine soils develop on the terrains of ice and snow, steppes, wetlands, alpine meadows and barren lands. The landscapes in subalpine areas include forests, meadows, steppes, semi-deserts and deserts. The piedmont hilly soil type appears in the desertified steppes and desert areas. The annual average runoff at the Yingluoxia Hydrological Station of the UHRB, with a total catchment area of 10,009 km$^2$, is $1.6 \times 10^{10}$ m$^3$, with unnoticeable intra-annual variability (Li et al., 2009) (Fig. 1).

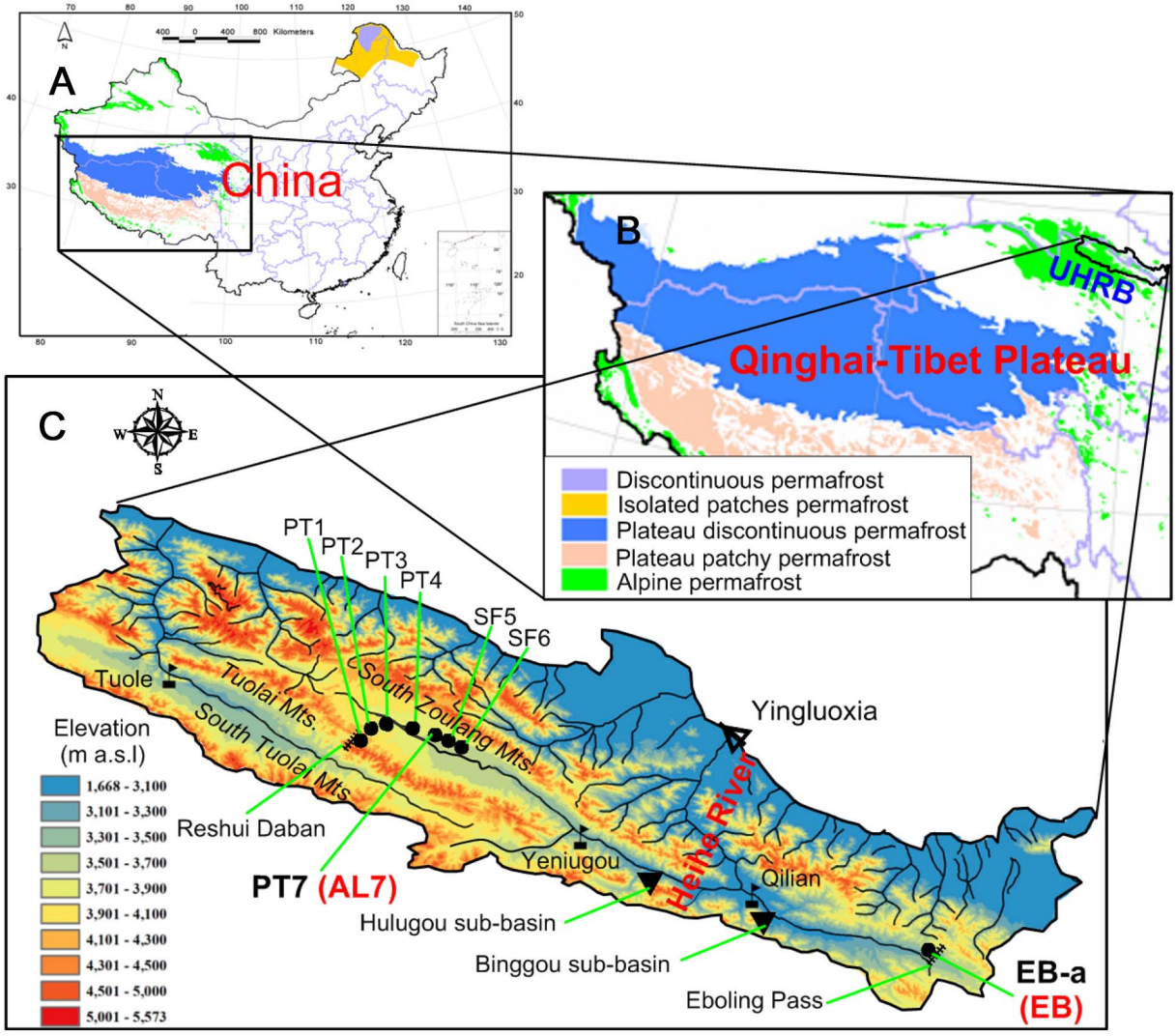


**Fig. 1.** Location of boreholes and active layer process sites in the UHRB.

### 2.2. Experimental design and data sources

In June and July 2011, seven boreholes (PT1, PT2, PT3, PT4, PT7, SF5 and SF6), with depths of 20 to 100 m, were drilled between the Reshui Daban (Pass) and the access road to the asbestos mine along the Qinghai Provincial Highway No. S204 on the alluvial plain at the western branch of the UHRB. Another borehole (EB-a), with a depth of 20 m, was drilled on the northern slope of the Eboling Mountains in late March 2012 (Fig. 1). Two observation sites for the active layer processes, AL7 and EB, were established in early October 2012, near the boreholes PT7 and EB-a, respectively, for monitoring soil temperatures and water contents in the active layer (Figs. 1–2). The EB site was located on a peatland on the northern slope of the Eboling Mountains. The vegetation type was alpine paludal meadow with 97% coverage by the dominant species of *Kobresia tibetica* Maximowicz, dotted with a number of turf hummocks. The AL7 site was located on an alluvial plain, covered by in alpine steppe with 80% coverage by the dominant species, *Kobresia pygmaea* C. B. Clarke (Fig. 2). Additional information on these two sites is shown in Table 1. The air temperatures at these sites were also observed starting in early October 2012.

Ground temperatures were monitored by thermometer cables permanently installed in boreholes, assembled and calibrated by the State Key Laboratory of Frozen Soils Engineering, with an accurate of better than 0.05 °C. The reading was taken manually at monthly intervals.

The temperatures and water contents of soils in the active layer were measured by using the 109 Temperature Probes and CS616 Water Content Reflectometer (Campbell Scientific, Inc.). The CR1000 data logger (Campbell Scientific, Inc.), powered by solar panels through batteries, was used for data acquisition. Lithology and installation depths of these soil temperature and water content probes at the AL7 and EB sites are shown in Fig. 3. It should be noted that only the volumetric content of unfrozen water could be measured by the CS616 probes. Air temperatures were measured by using the HOBO Pro V2 (U23) (Onset Computer Corporation) placed in a thermometer shelter. The range and error of the above-described instruments were presented by Wang et al. (2016b). All of the observation steps were set at 30 min in duration.

In order to compare the difference in hydrothermal processes of soils in the active layer for the EB and AL7 sites, ΔT, ΔW, the freezing index (FI) and the thawing index (TI) of soils in the active layer are calculated using following formulas:

$$\Delta T_i = T_{EB,i} - T_{AL7,i} \quad (1)$$

$$\Delta W_i = W_{EB,i} - W_{AL7,i} \quad (2)$$

where $\Delta T_i$ and $\Delta W_i$ are the difference in soil temperature and water content for the EB and AL7 sites, respectively; the *i* is the depth number of soil temperature and water content in the active layer.

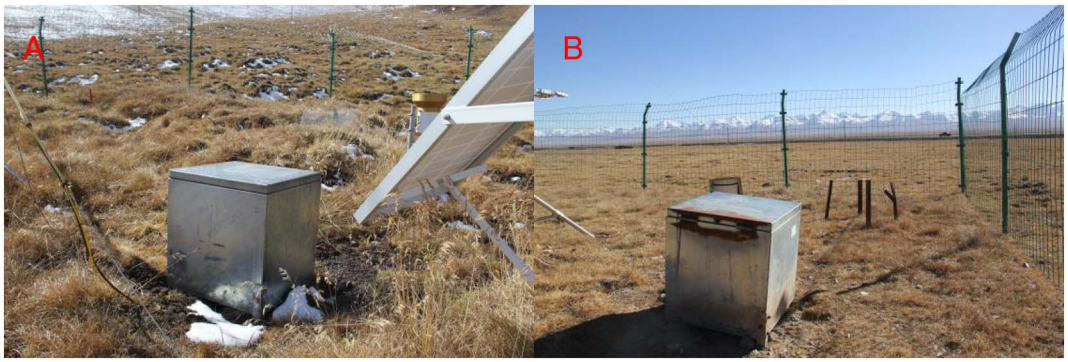


**Fig. 2.** Photos of the EB (A) and AL7 (B) active layer process sites.

$$FI = \sum_{i=1}^{N_F} |T_i|,\ T_i < 0^{\circ}\mathrm{C} \tag{3}$$

where FI is the freezing index of soils in the active layer; the $i$ is the day number when the daily soil temperature is below freezing, $i = 1, 2, \ldots N_F$.

$$TI = \sum_{i=1}^{N_T} |T_i|,\ T_i > 0^{\circ}\mathrm{C} \tag{4}$$

where TI is the thawing index of soils in the active layer; the $i$ is the day number when the daily soil temperature is above freezing, $i = 1, 2, \ldots N_T$.

Dry density and moisture contents of soils (percent by mass, as measured by the oven drying) from wellbores were determined at the Key Laboratory of Western China's Environmental Systems (Ministry of Education), Lanzhou University. The MAATs at the Qilian, Yeniugou and Tuole meteorological stations in the UHRB were calculated for the period from 1955 to 2015 based on monthly air temperatures provided by the China Meteorological Administration.

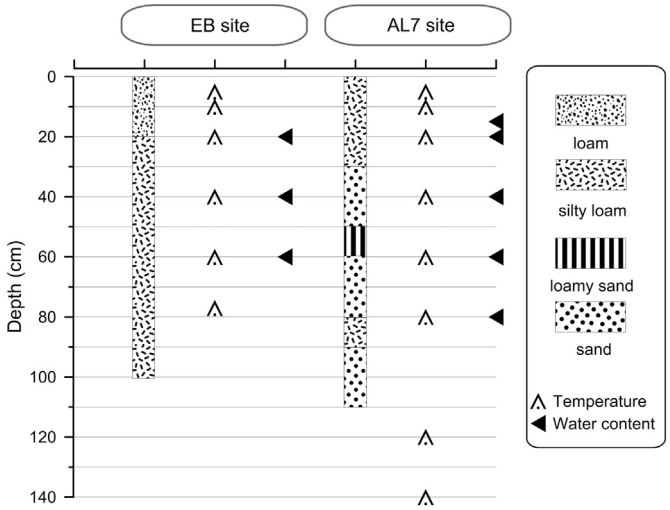


**Fig. 3.** Lithology and installation depths of soil temperature and water content probes at the EB and AL7 active layer process sites.

## 3. Results

### 3.1. LLP and other features of permafrost in the UHRB

With a decreasing elevation from 4132 m to 3700 m a.s.l., the MAGT increased gradually from − 1.8 °C (at borehole PT1) to − 0.1 °C (at borehole PT5) at the western branch of the UHRB, and the permafrost thinned from > 100 m to ~12 m. The MAGT was 0.7 °C at an elevation of 3649 m a.s.l., and 2.1 °C at an elevation of 3609 m a.s.l. Seasonally frozen ground occurred at boreholes SF5 and SF6 (Fig. 4). When synthesized with the data from previous geophysical sounding and pit excavations, these measurements indicated a LLP at elevations between 3650 m and 3700 m a.s.l. on the alluvial plain at the western branch of the UHRB. At similar elevations, permafrost was absent on the southern slope of the Eboling Mountains at the eastern branch. On the northern slope of the Eboling Mountains, the LLP was at an elevation of 3600 m a.s.l. However, occasionally islanded patches permafrost occurred at elevations of above 3400 m a.s.l. under very favourable conditions.

The ground temperature profile of borehole PT5 showed a permafrost thickness of ~12 m. At about the same elevation on the northern slope of the Eboling Mountains, measurements from the borehole EB-a indicated a permafrost thickness of > 20 m, due to the zero geothermal gradient at depths below 7 m. The ground temperatures at depths of 2 to 20 m at borehole EB-a were 0.5 to 0.9 °C lower than those at borehole PT5 (Fig. 4). It is thus estimated that the northern slope of the Eboling Mountains have a thicker permafrost and a lower MAGT than areas of the similar elevations. Although the MAAT at the EB site was 1.7 °C higher than that at the AL7 site, the mean annual soil temperatures (MASTs) at depths of 5–77 cm in the active layer were 0.6–1.5 °C lower than those at the AL7 site (Fig. 10). These findings raised

**Table 1**
Metadata for the EB and AL7 active layer process sites in the alpine permafrost region in the UHRB.

| Sites | Lat. /Long. | Elev. (m a.s.l.) | MAAT(°C) | $ARST_5$ (°C) | ALT (m) | MAGT (°C) | Vegetation type |
|---|---|---|---|---|---|---|---|
| EB | 100°54.98′ E 37°59.87′ N | 3691 | − 2.4 | 19.6 | 0.8 | − 0.8 | alpine paludal meadow |
| AL7 | 99°1.55′ E 38°48.33′ N | 3700 | − 4.1 | 28.4 | 3.9 | − 0.1 | alpine steppe |

$ARST_5$ is annual range of soil temperature (ARST) at a depth of 5 cm.
ALT, active layer thickness.
MAGT, mean annual ground temperature at a depth of 14 m.
MAAT and $ARST_5$ are calculated from the daily data collected from 1 January to 31 December 2013.

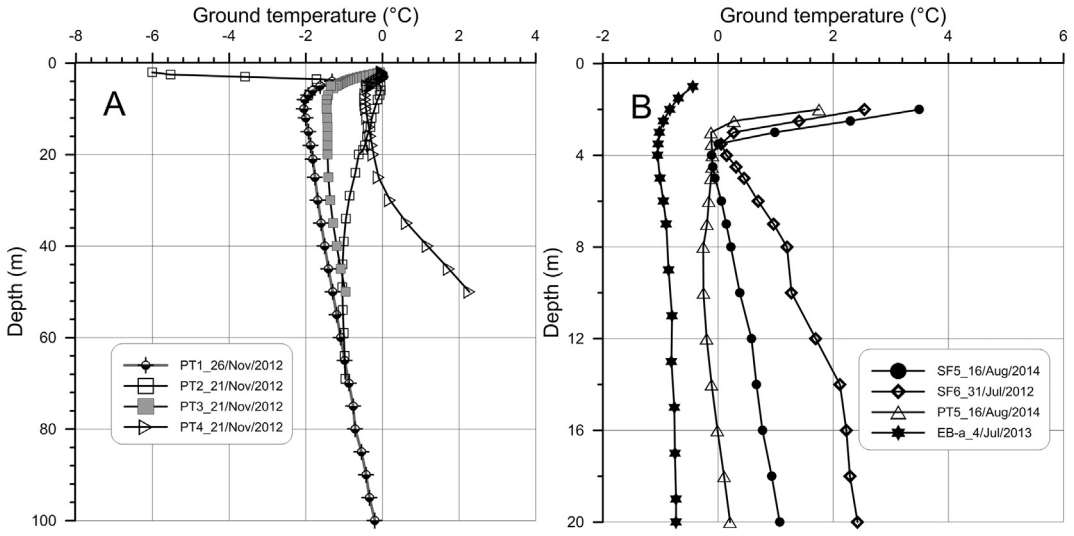


**Fig. 4.** Ground temperature profiles at boreholes in the UHRB in 2012–2014.

questions concerning the reasons for these relationships between ground and air temperatures at the two sites.

### 3.2. Hydrothermal processes of soils in the active layer in the UHRB

#### 3.2.1. Seasonal divisions of freeze-thaw processes of soils in the active layer

The hydrothermal processes of soils in the active layer can be divided into the thaw process (TP), freeze process (FP), cooling process (CP) and warming process (WP) (Hinkel and Nicholas, 1995; Osterkamp and Romanovsky, 1997; Romanovsky and Osterkamp, 1997; Zhao et al., 2000; Hinkel et al., 2001; Wang et al., 2009b, 2012). To be specific, at the EB and AL7 sites, the CP lasts from the end of November or early December to early March of the next year. The WP is the period between the end of CP and the onset date for ground thaw. The TP extends from the onset date of ground thaw (from the ground surface downward) in late or mid-April, through the date when the active layer reaches its maximum depth in late October. The FP consists of the time between the date when the active layer reaches its maximum depth and the date on which the entire active layer is frozen up (Zhao et al., 2000) (Fig. 5).

#### 3.2.2. Dynamics of soil temperature and water content in the active layer

At the EB and AL7 sites, soil temperatures showed a trend of decreasing seasonal variability with the increase of depth from 5 to 77 cm. At the EB site, soil temperatures generally reached their lowest values in late January to late February, and the highest values from early July to early October. However, at the AL7 site, soil temperatures generally reached their lowest values in mid-January, and highest in early July to late August. Soil temperatures at depths of 5 to 77 cm at the EB site were lower in the warm season and higher in the cold season than those at the AL7 site. In other words, the ΔT was negative in the warm season and positive in the cold season. The duration with higher soil temperatures at depths of 5 to 77 cm at the EB site than those at the AL7 site (i.e., $\Delta T > 0$ °C) accounted for < 1/3 of the year. In addition, the absolute value of ΔT at deeper depths (20–77 cm) was greater than that at shallower depths (5–10 cm) in the warm season (Fig. 6).

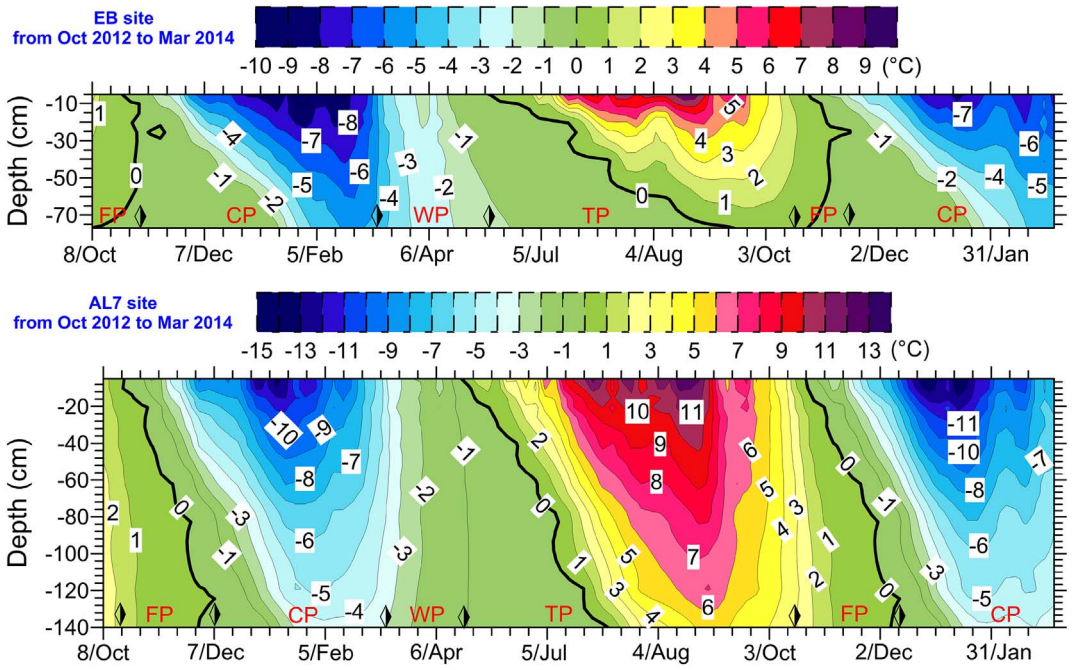


**Fig. 5.** Contour map of active layer soil temperatures at the EB and AL7 sites from 8 October 2012 to 6 March 2014, and the periods of seasonal freeze-thaw processes.

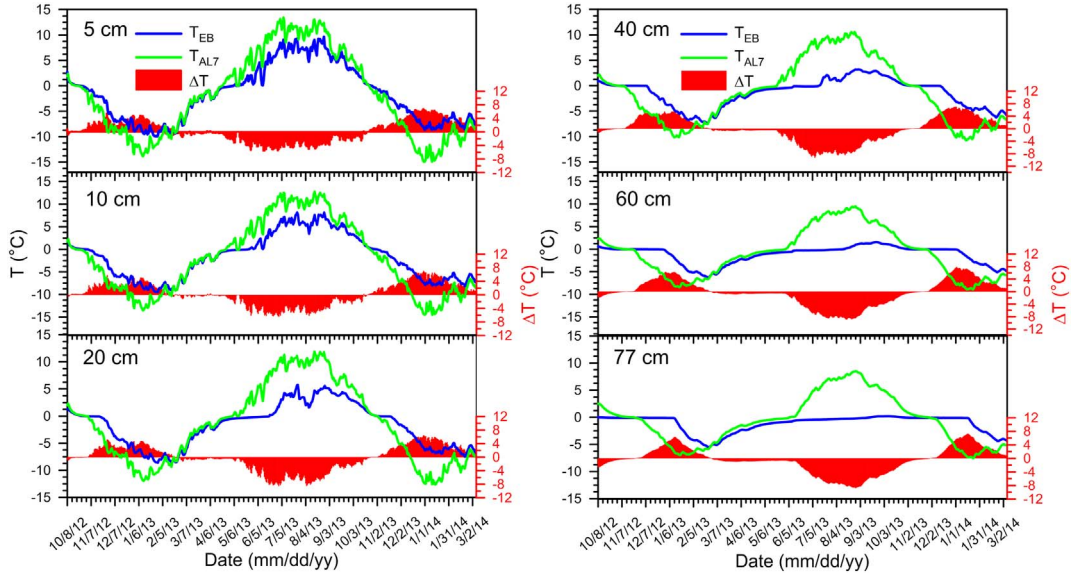


**Fig. 6.** Soil temperature dynamics in the active layer at different depths at the EB and AL7 sites from 8 October 2012 to 6 March 2014.
Notes:
Soil temperature at a depth of 77 cm at the AL7 site is linearly interpolated according to the soil temperatures at depths of 60 cm and 80 cm.

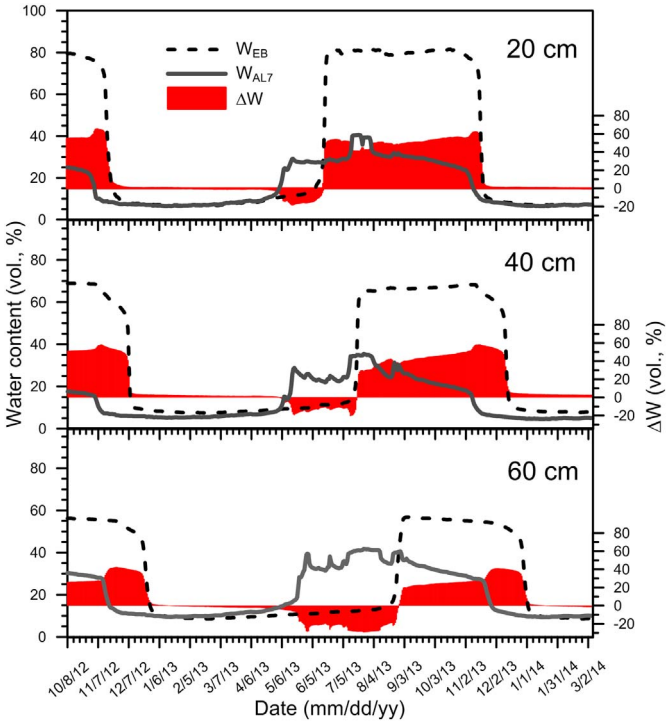


**Fig. 7.** Dynamics of soil water contents at different depths of 20, 40 and 60 cm in the active layer at the EB and AL7 sites from 8 October 2012 to 6 March 2014.

Soil water contents at depths of 20 to 60 cm at the EB and AL7 site were higher in the warm season and lower in the cold season. From early May to late August, soil water contents at depths of 20 to 60 cm at the EB site were significantly lower than those at the AL7 site (i.e., $\Delta W < 0$). Moreover, the durations of the negative ΔW at a depth of 60 cm were much longer than those at depths of 20 to 40 cm (Fig. 7).

## 4. Discussions

### 4.1. Influences of the thermophysical properties and moisture contents on active layer hydro-thermal processes

The seasonal freeze-thaw processes in the active layer are closely related to the thermophysical properties of soils, such as soil compositions, dry density, porosity and moisture contents (Zhou et al., 2000). The thermal conductivity, diffusivity and volumetric heat capacity of soils are closely related to dry density and moisture contents of soils (Zhou et al., 2000). The dry density of soils at the EB and AL7 sites varied from 0.25–0.67 to 0.86–1.91 g $cm^{-3}$, respectively. The soil moisture contents varied between 63% and 83% at the EB site, and from 4.7% to 16.7% at the AL7 site, with the means at 75.6% and 8.1%, respectively (Fig. 8). When the dry density and moisture content of soils are same, the thermal conductivity and diffusivity of the coarse soils are larger and the specific heat is smaller than those of the fine soils. In the fine-grained soils, the thermal conductivity and diffusivity of peat is smallest, and specific heat is largest (Zhou et al., 2000). This may explain for the thawing rate and maximum thawing depth in the active layer at the EB site of one-fifth those at the AL7 site (Fig. 5). It also results in the lower soil temperatures at depths of 5–77 cm in the active layer at the EB site in the warm season and the higher soil temperatures in the cold season than those at the AL7 site (Fig. 6).

Moreover, in the warm season, the soil water contents in the active layer at the EB site on peatlands were significantly higher than those at the AL7 site, especially at the deeper depths (20–60 cm) (Fig. 7). The high specific heat of the water (4.12 KJ $kg^{-1}$ $K^{-1}$) also results in the lower soil temperatures in the active layer at the EB site in the warm season than those at the AL7 site, especially at deeper depths (20–77 cm) (Fig. 6).

As the temperature rose after lowering to its lowest value at the beginning of the year, the air was warmer than ground, and the active layer began to absorb heat from the atmosphere. In other words, this was the WP of active layer. The heat conduction dominated in the frozen-up active layer, and there was a convective heat transfer of both liquid water (i.e., unfrozen water) and gaseous water (vapor), due to the temperature and solute concentration gradients (Xu et al., 2010). Ice-rich peat needed to absorb large amount of heat upon thawing. Therefore, at the EB site, soil temperatures at depths between 5 and 77 cm were lower than those at the AL7 site during the WP (Fig. 6).

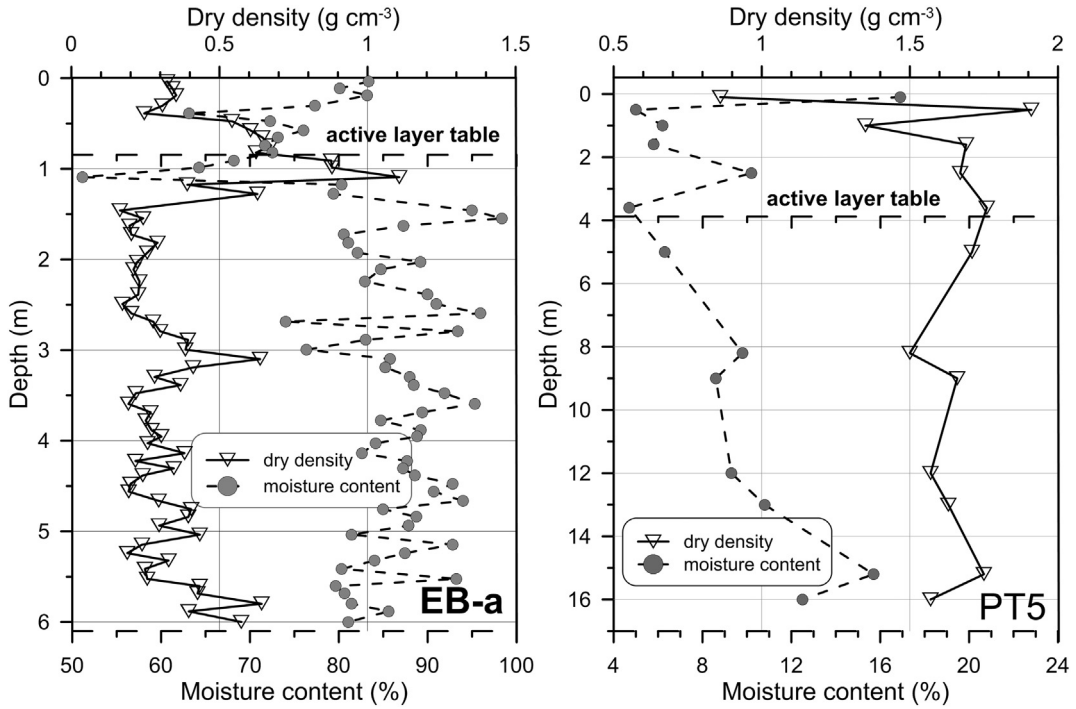


**Fig. 8.** Dry density and moisture contents of soils at depths of 0–6 m in Borehole EB-a (A) and at depths of 0–16 m in Borehole PT5 (B).

As surface temperature gradually increased to ~0 °C and continued to rise, the active layer began to thaw unsteadily, and then moved to a stable progressive top-down thaw. Unlike at the AL7 site, soil temperature at the EB site, especially at the depth of 77 cm, remained at 0 °C for a long period during the TP (i.e., zero curtain), mainly because the phase transitions of ice to water (Fig. 5). Near-surface ground temperatures were more susceptible to precipitation and surface evapotranspiration at the AL7 site. At the EB site, the thermal effects of precipitation on soil temperatures were significantly less, due to its wet or saturated peatland soils in the active layer (Fig. 6). Moreover, because of the thermophysical properties and water contents of peat soils, the ΔW at depths of 20 to 60 cm was negative from early May to late August, and the duration of negative ΔW at the depth of 60 cm was much longer than those at depths of 20 to 40 cm (Figs. 7).

Unlike the freeze process of seasonally frozen ground, the 2-directional freezing process (i.e., downward and upward) was observed in the active layer (Zhou et al., 2000). At the EB site, the thickness by the downward ground freezing (of 45 cm) and freezing rate (of 4.5 cm/d) were both significantly greater than those of the upward freezing thickness (25 cm) and freezing rate (2.1 cm/d). In the seasonal thaw layer at the EB site, the downward and upward freeze layers accounted for ~64% and 36% of the active layer thickness, respectively. At the AL7 site, the downward freeze rate was 2.8 cm/d at depths of 5 to 140 cm (Fig. 5).

In general, soil moisture migrated from downward due to gravity, although there were contrary tendencies including top-down migration of free water, upward migration of capillary water, evapotranspiration and convection of water vapor in the thaw layer (Hinkel and Nicholas, 1995), and downward migration of unfrozen water in the frozen layers (Zhao et al., 2000). In the thaw layer, both heat conduction and convection (i.e., free and forced convection modes) were active, but heat conduction was dominant in the frozen layer (Zhao et al., 2000).

In this study, 0 °C is regarded as the freezing and thawing temperature of soils and water at the EB and AL7 sites. However, soil generally doesn't freeze (or thaw) at a temperature of 0 °C in nature. Therefore, for determining the division between the freeze-thaw processes in the active layer and hydro-thermal dynamics, it is crucial to carry out laboratory tests to more accurately determine the freezing and thawing temperatures for soils at the EB and AL7 sites.

### 4.2. Thermal diode properties of peat soils

The unique thermophysical properties of peat soils led to lower soil temperature in the warm season and higher soil temperature in the cold season. In the warm season, the greater absolute value of ΔT at deeper depths (20–77 cm) than that at shallower depths (5–10 cm) was also related to ice melting in the active layer on peatlands (Fig. 6). In the active layer at the EB site on peatlands, the FI and TI of soils were lower at depths of 5 to 77 cm than those at the AL7 site. The FI and TI of soils both decreased with increasing depth (Fig. 9A, D). This trend showed that the heat exchange between ground and air decayed with the increasing depth in the active layer. It is worth mentioning that the TI of soils at depths of 60 and 77 cm at the EB site were much lower than those at depths of 5 to 40 cm (Fig. 9D). There could be two main reasons for this pattern. First, the heat absorption rate of peatlands was slower, as peatlands had a higher specific heat and lower thermal conductivity and diffusivity. Second, surface evapotranspiration consumed large amount of latent heat in the wet or saturated surface peatlands, and the ice-rich soil, especially near the permafrost table, would absorb large amount of latent heat.

In addition, at the EB site, the mean temperatures of soils at depths of 5 to 77 cm during periods with subzero and above-zero temperatures were both significantly lower than those at the AL7 site (Fig. 9B, E). Duration of periods with subzero soil temperatures was longer than that with above-zero soil temperatures, especially at the EB site (Fig. 9C, F). The FI/TI ratios of soils at the EB site were significantly higher than those at the AL7 site, with the values being 1.2–75.1 and 0.7–0.9, respectively (Fig. 9A, C). These findings indicated that over the course of observations over a year, the active layer was mainly exothermic at the EB site, but endothermic at the AL7 site. This pattern was best demonstrated by the ARSTs and MASTs of the active layers. The ARSTs and MASTs at the EB site were smaller than those at the AL7 site, with the ARSTs being 4.8 to 16.6 °C and 8.5 to 23.4 °C, respectively, and the MASTs being − 1.2 to − 0.3 °C and 0.2 to 0.5 °C, respectively (Fig. 10).

It was also found that at the EB site, the freeze-thaw cycle in soils led to an enhanced heat loss in the active layer on peatlands, which

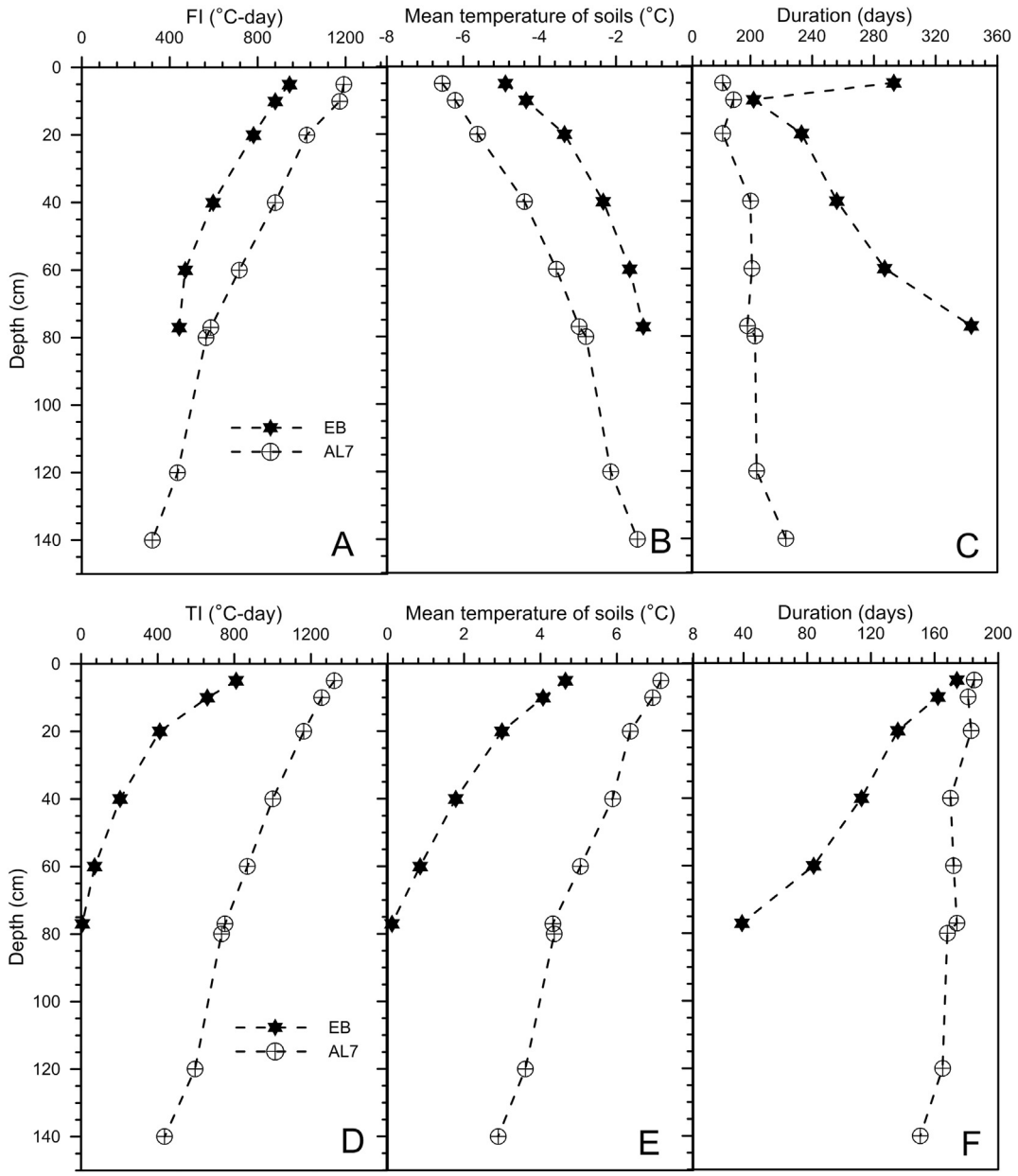


**Fig. 9.** The FI, TI, the mean temperature of soils during periods with subzero and above-zero temperatures, and duration of periods with subzero and above-zero soil temperatures at different depths in the active layer at the EB and AL7 sites in the cold and warm seasons from 8 October 2012 to 31 December 2013.
Note:

showed unique thermophysical properties of reduced heat absorption in the warm season and of reduced heat release in the cold season. That is, the active layer helped in preserving the underlying permafrost on peatlands.

(A) FI (freezing index);
(B) Mean temperature of soils during periods with subzero temperatures;
(C) Duration of periods with subzero soil temperatures;
(D) TI (thawing index);
(E) Mean temperature of soils during periods with above-zero temperatures;
(F) Durations of periods with above-zero soil temperatures.

### 4.3. Permafrost degradation and its possible eco-hydrological impacts

From 1957 to 2015, the MAATs at the Qilian, Yeniugou and Tuole meteorological stations in the UHRB have all shown significant trends of climate warming, with the average rate being 0.27–0.35 °C/10a ($p < 0.05$) (Fig. 11). Based on distributed air temperature data with an 1-km spatial resolution, adjusted by the air temperature lapse rate of 6 °C/km, it was calculated that the MAATs exhibited a significant upward trend from 1961 to 2014 in the Qilian Mountains, with the rate being 0.34 °C/10a ($p < 0.05$) (Qin et al., 2016) (Fig. 11). This result was consistent with the observation data collected at the three meteorological stations in the UHRB and the adjacent areas.

In addition, observation and simulation results of previous studies showed increasing soil temperatures in the Qilian Mountains; the onset dates of ground freezing were delayed; the end dates of ground freezing advanced; the maximum depth of seasonal frost penetration declined (especially near the LLP) (Wang et al., 2015a); the leaf area index increased (Qin et al., 2016); and the vegetation green-up date advanced (Zhang et al., 2013b). By assuming a lapse-rate of air temperature at 6 °C/km and a warming rate of 0.3 °C/10a, it was calculated that

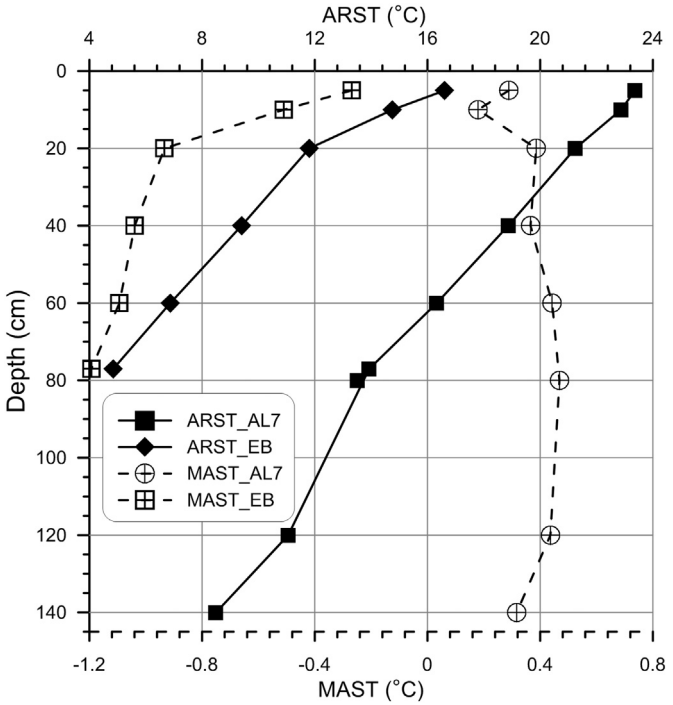


**Fig. 10.** ARSTs and MASTs of the active layer soils at the EB and AL7 sites from 1 January to 31 December 2013.

30 years ago (i.e., in 1985), the LLP on the alluvial plain was at ~3500–3550 m a.s.l. This calculation was consistent with the conclusion drawn by Guo and Cheng (1983) that the LLP permafrost was at 3450–3650 m a.s.l. in the Lenglongling Mountains, South Zoulang Mountains and on the northern slope of the Qilian Mountains. In other words, the LLP has elevated by 100–200 m and the permafrost zone has shrunk by 10–20 km along the major highways since 1985, and permafrost will continue to degrade by ~15 to 25 km along the highways by 2045. Therefore, it can be deduced that the LLP on the alluvial plain will rise to 3750–3800 m a.s.l. by 2035, to 3800–3850 m a.s.l. by 2045 and to 3850–3900 m a.s.l. by 2055. This projection indicates that permafrost may disappear on the alluvial plain at the western branch of the UHRB after 40 years.

On the northern slope of the Eboling Mountains at the eastern branch of the UHRB, the LLP was at 3600 m a.s.l., and isolated patches of permafrost was still found at 3400 m a.s.l. This finding was consistent with the results by Zhu et al. (1996) and Wu et al. (2007). However, unlike the explanations given by Zhu et al. (1996) and Wu et al. (2007), there could be two main reasons for the basically unchanged LLP over the previous 20 years. One reason is the unique thermal diode property of the active layer soils on peatlands, which has a protective effect on the underlying permafrost. Additionally, permafrost is ice-rich on peatlands. The average soil moisture content in the permafrost layer at the borehole EB-a was as high as 86.7%, but that at the borehole PT5 was only 10.4%. This set of findings indicate that the soil moisture contents in the permafrost layer at the borehole EB-a was 7 times higher than that at the borehole PT5 (Fig. 8).

Permafrost is ice-rich on the northern slope of the Eboling Mountains, and the phase change of ground ice requires absorbing large amount of heat, thereby causing the so-called “latent heat effects”. However, permafrost at the western branch alluvial plain is ice-poor (Fig. 8), and it is therefore more susceptible to climate change, which may lead to a more rapid elevation of the LLP. As shown by other observation results in the Arctic, Sub-Arctic and on the QTP, warming rates are much higher for cold permafrost than warm ($> -1$ °C) permafrost, and this trend in warming rates are especially prevalent for ice-rich permafrost (e.g., Cheng and Wu, 2007; Romanovsky et al., 2010; Smith et al., 2010; Wu et al., 2016).

Based on a study of marshes and permafrost in the Xing'an Mountains in Northeastern China, Jin et al. (2008) proposed a mechanism of symbiosis between swamp and permafrost. This principle is also applicable in the alpine permafrost regions on northeastern QTP. In addition, the northern slope of the Eboling Mountains, on the windward slope of the winter monsoon, is susceptible to the frequent invasions of cold air masses, and the surface snow-melting in spring has a protective effect on the underlying active layer and permafrost. However, a medium-scale retrogressive slump, with a length of ~3 km, several metres wide and ~2.5 m deep, has occurred in recent decades on the peatlands on the northern slope of the Eboling Mountains (Fig. 12). The slump indicates a more rapid permafrost degradation and will certainly affect the eco-hydrological processes of the peatlands.

Under a warming climate, permafrost degradation and subsequent deepening active layer have led to enhanced infiltration and greater storage capacity of the suprapermafrost water in the active layer. These changes have resulted in reduced surface runoffs, and increased base flow in winter (e.g., Serreze et al., 2000; Zhang et al., 2005; Ye et al., 2009; Niu et al., 2011; Zhang et al., 2013c; Wang et al., 2015b; Qin et al., 2016). Chen et al. (2014) concluded that the uplift of cold regions vegetation zones caused by climate warming could result in a higher ratio of evapotranspiration to precipitation and smaller runoff

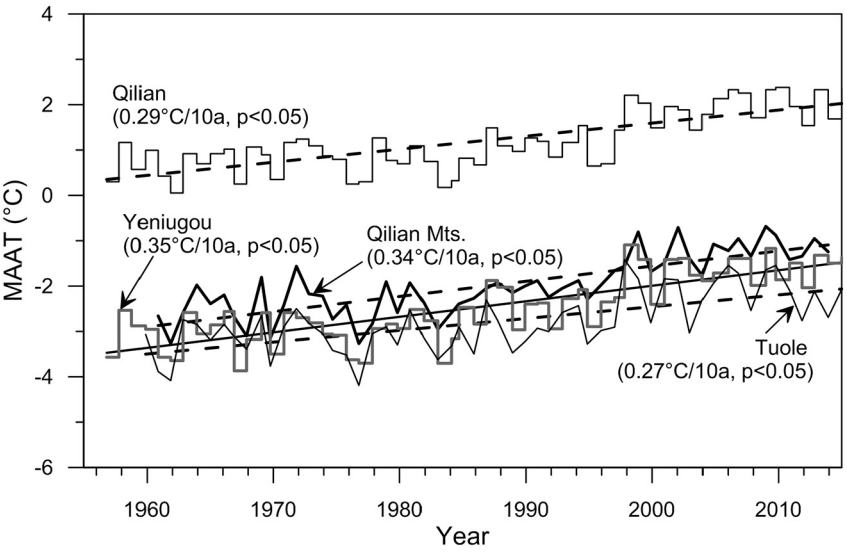


**Fig. 11.** Interannual variations in the MAAT and its trends at the Qilian, Yeniugou and Tuole meteorological stations in the UHRB from 1957 to 2015 and in the Qilian Mountains from 1961 to 2014 (Qin et al., 2016).

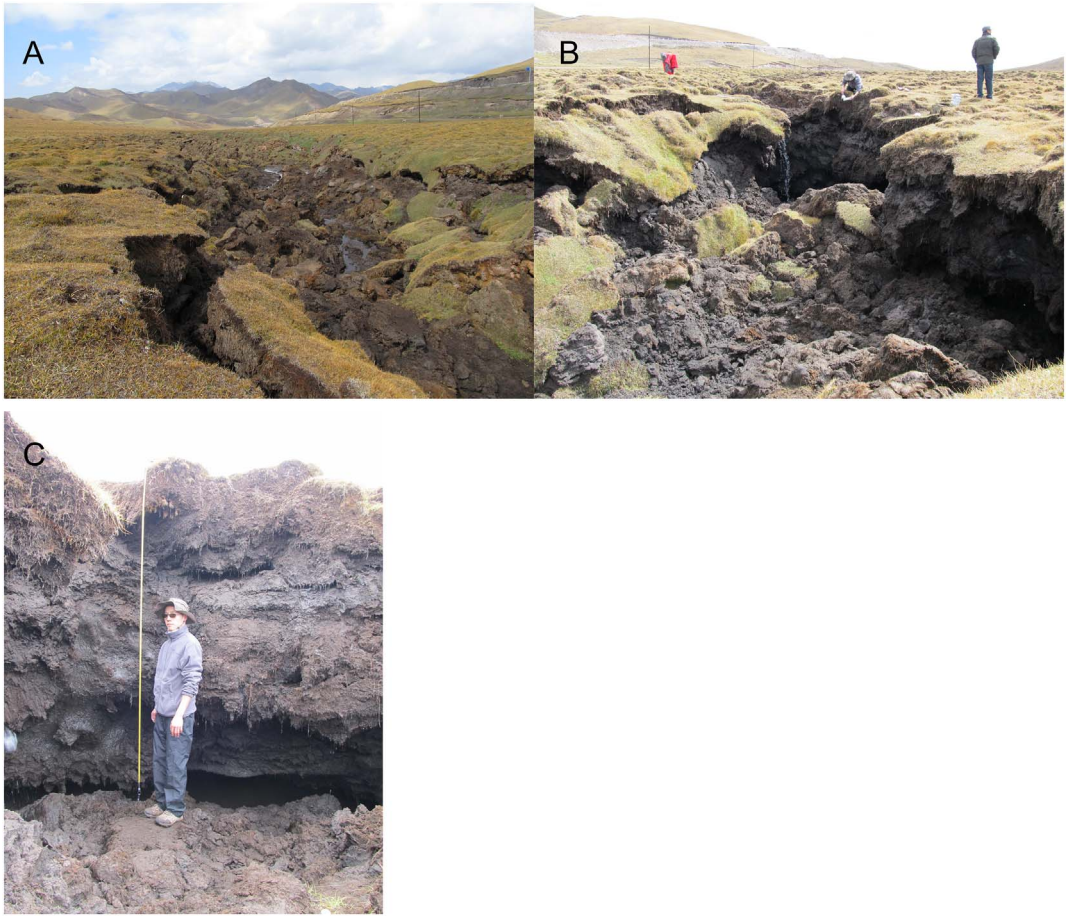


**Fig. 12.** Retrogressive thaw slumps on the northern slope of the Eboling Mountains in the UHRB.
Note:
(A) Retrogressive thaw slumps seen from the higher elevation to the lower elevation;
(B) The source of retrogressive thaw slumps;
(C) The depth of retrogressive thaw slumps.

coefficients. Ye et al. (2009) and Niu et al. (2011) explained that the hydrological impacts of permafrost degradation were also related to the areal extent of permafrost in a watershed.

In addition, Chen and Han (2010) and Chen et al. (2014) urged that the alpine cold desert zone, which is considered to be the main runoff area in the UHRB, should be more systematically observed and studied. Other researchers have recommended that the influences of snow cover on the hydrological processes in the active layer on north-facing slope should be closely examined (e.g., Zhang et al., 2013c; Zhou et al., 2013, 2014). However, so far they are still very limited or absent in major Chinese mountains.

In conclusion, there is no doubt that the degradation of frozen ground due to climate warming and increased human activities has extensively affected the eco-hydrogeological environment in cold regions. However, the specific and quantitative effects of frozen ground degradation on the hydrological processes of watersheds have remained unclear. Therefore, there is an urgent need to strengthen systematic, long-term observations and research on the hydrological functions of different landscapes in alpine permafrost regions. Only such efforts can allow scientists to more systematically and scientifically evaluate and more correctly predict the hydrological impacts of changing frozen ground.

## 5. Conclusions

Based on careful measurements of ground temperatures in boreholes, of soil temperatures and water contents in the active layer and of the MAATs at the Qilian, Yeniugou and Tuole meteorological stations in the UHRB and the adjacent areas, a series of observations were made regarding changes in the LLP and the related hydrothermal dynamics in the active layer and permafrost. Analyses were conducted on the possible eco-hydrological impacts from the degrading permafrost.

The main conclusions from this investigation are drawn as follows:

(1) The LLP was now at 3650–3700 m a.s.l. on the alluvial plain at the western branch of the UHRB in the Qilian Mountains. However, permafrost was absent on the southern slope of Eboling at the eastern branch. On the northern slope of the Eboling Mountains, the LLP was at 3600 m and 3400 m a.s.l., although isolated patches of permafrost could be occasionally encountered at lower elevations until 3400 m a.s.l.

(2) Soil temperatures at depths of 5 to 77 cm were lower in the warm season and higher in the cold season near the LLP on the northern slope of the Eboling Mountains than those at the LLP at the western branch of the UHRB. In the warm season, the absolute value of $\Delta T$ at deeper depths (20–77 cm) was greater than that at shallower depths (5–10 cm). The $\Delta W$ at the depths of 20 to 60 cm was negative from early May to late August, and the duration of the negative $\Delta W$ at the depth of 60 cm was much longer than those at the depths of 20 to 40 cm.

(3) Because of the thermal diode effect of peat soils, the thaw rate and downward freeze rate of the active layer on peatlands near the LLP on the northern slope in the Eboling Mountains were 0.2 and 1.6 times those found at the LLP at the western branch of the UHRB; the ARSTs and MASTs of the active layer on the peatlands and the MAGT were all

significantly lower. In short, peatland soils have unique thermophysical properties, which help reduce heat releasing in the cold season, and reduce heat absorption in the warm season. These properties of peatlands also make the underlying permafrost with a lower temperature.

(4) The FI and TI of soils at depths of 5 to 77 cm in active layer were smaller near the LLP on the northern slope in the Eboling Mountains than those at the LLP at the western branch of the UHRB. With increasing depth, the FI and TI of soils at the two sites decreased. In addition, the FI/TI ratios of soils near the LLP on the northern slope in the Eboling Mountains were significantly larger than those at the LLP at the western branch of the UHRB.

## Acknowledgments

We appreciate for Reviewers' insightful comments and constructive suggestions. And we thank Dr. Jichun Wu for his helpful suggestions on revision manuscript. This study is supported by the Key Research Program of the Chinese Academy of Sciences (CAS) (Grant No. KZZD-EW-13), National Natural Science Foundation of China (Grant Nos. 91325202, and 41501080), Talent Fund of Cold and Arid Regions Environmental and Engineering Research Institute, CAS (Grant No. 51Y551D71), and Research Project of State Key Laboratory of the Frozen Soil Engineering (Grant Nos. 52Y452F21 and 52Y652J11), China Postdoctoral Science Foundation Project (2016 M602900), and Fundamental Research Funds for the Central Universities (Grant No. lzujbky-2015-123).

## References

Arctic Climate Impact Assessment (ACIA), 2005. Impacts of a Warming Climate. Cambridge University Press, Cambridge (144 pp.).

Bense, V.F., Ferguson, G., Kooi, H., 2009. Evolution of shallow groundwater flow systems in areas of degrading permafrost. Geophys. Res. Lett. 36. http://dx.doi.org/10.1029/2009GL039225.

Bense, V.F., Kooi, H., Ferguson, G., Read, T., 2012. Permafrost degradation as a control on hydrogeological regime shifts in a warming climate. J. Geophys. Res. 117. http://dx.doi.org/10.1029/2011JF002143.

Cao, W.B., Wan, L., Zhou, X., Hu, F.S., Li, Z.M., Liang, S.H., 2003. A study of the geological environment of superapermafrost water in the headwater of the Yellow River. Hydrogeol. & Eng. Geol. 6, 6–10 (in Chinese).

Cao, B., Gruber, S., Zhang, T., Li, L., Peng, X., Wang, K., Zheng, L., Shao, W., Guo, H., 2017. Spatial variability of active layer thickness detected by ground penetrating radar in the Qilian Mountains, Western China. J. Geophys. Res. 122, 574–591.

Carey, S.K., Woo, M.K., 2001. Slope runoff processes and flow generation in a subarctic, subalpine catchment. J. Hydrol. 253 (1–4), 110–129.

Chen, R.S., Han, C.T., 2010. Hydrology, ecology and climate significance and its research process of the alpine cold desert. Adv. Earth Science 25 (3), 255–263 (in Chinese).

Chen, R.S., Yang, Y., Han, C.T., Liu, J.F., Kang, E.S., Song, Y.X., Liu, Z.W., 2014. Field experimental research on hydrological function over several typical underlying surfaces in the cold regions of western China. Adv. Earth Science 29 (4), 507–514 (in Chinese).

Cheng, G.D., Jin, H.J., 2013. Permafrost and groundwater on the Qinghai-Tibet plateau and in northeast China. Hydrogeol. J. 21, 5–23.

Cheng, G.D., Wu, T.H., 2007. Responses of permafrost to climate change and their environmental significance, Qinghai-Tibet Plateau. J. Geophys. Res. 112 (F02S03). http://dx.doi.org/10.1029/2006JF000631.

Cheng, G.D., Zhou, Y.W., 1988. State of the art and prospect of geocryology in China. J. Glaciol. Geocryol. 10 (3), 221–227 (in Chinese).

Ding, Y.J., Xiao, C.D., 2013. Challenges in the study of cryospher-ic changes and their impacts. Adv. Earth Science 28 (10), 1067–1076 (in Chinese).

Gao, T.G., Zhang, T.J., Lan, C., Kang, S.C., Sillanpää, M., 2016. Reduced winter runoff in a mountainous permafrost region in the northern Tibetan Plateau. Cold Reg. Sci. Technol. 126, 36–43.

Gruber, S., Haeberli, W., 2009. Mountain permafrost, permafrost soils. Spring 33–44.

Guo, P.F., Cheng, G.D., 1983. Zonation and formation history of permafrost in Qilian Mountains of China. In: Proc 4th Int. Conf. on Permafr., Washington D.C. Vol I (395–340).

Hinkel, K.M., Nicholas, J.R.J., 1995. Active layer thaw rate at a boreal forest site in central Alaska, USA. Arct. Alp. Res. 27, 72–80.

Hinkel, K.M., Paetzold, F., Nelson, F.E., Bockheim, J.G., 2001. Patterns of soil temperature and moisture in the active layer and upper permafrost at Barrow, Alaska: 1993–1999. Glob. Planet. Chang. 29, 293–309.

Hinzman, L.D., Bettez, N., Chapin, F.S., Dyurgerov, M., Fastie, C., Griffith, D.B., Hope, A., Huntington, H.P., Jensen, A., Kane, D.L., Kofinas, G., Lynch, A., Lloyd, A., McGuire, A.D., Nelson, F.E., Osterkamp, T., Oechel, W.C., Racine, C., Romanovsky, V.E., Schimel, J., Stow, D., Sturm, M., Tweedie, C.E., Vourlitis, G., Walker, M., Webber, P.J., Welker, J., Winker, K., Yoshikawa, K., 2005. Evidence and implications of recent climate change in terrestrial regions of the Arctic. Clim. Chang. 72, 251–298.

Jin, H.J., Li, S.X., Cheng, G.D., Wang, S.L., Li, X., 2000. Permafrost and climatic change in China. Glob. Planet. Chang. 26, 387–404.

Jin, H.J., Zhao, L., Li, S.X., Wang, S.L., Jin, R., 2006. Thermal regimes and degradation modes of permafrost along the Qinghai-Tibet Highway. Sci. China Ser. D Earth Sci. 49 (11), 1170–1183.

Jin, H.J., Sun, G.Y., Yu, S.P., He, R.X., 2008. Symbiosis of marshes and permafrost in Da and Xiao Hinggan Mountains in northeastern China. Chin. Geogr. Sci. 18 (1), 062–069.

Jorgenson, M.T., Racine, C.H., Walters, J.C., Osterkamp, T.E., 2001. Permafrost degradation and ecological changes associated with a warming climate in central Alaska. Clim. Chang. 48, 551–579.

Jorgenson, M.T., Shur, Y.L., Pullman, E.R., 2006. Abrupt increase in permafrost degradation in Arctic Alaska. Geophys. Res. Lett. 33 (2).

Kang, E.S., Chen, R.S., Zhang, Z.H., Ji, X.B., Jin, B.W., 2008. Some problems facing hydrological and ecological researches in the mountain watershed in the upper stream of an inland river basin. Adv. Earth Science 23, 675–681 (in Chinese).

Lan, C., Zhang, Y.X., Bohn, T.J., Zhao, L., Li, J.L., Liu, Q.M., Zhou, B.R., 2015. Frozen soil degradation and its effects on surface hydrology in the northern Tibetan Plateau. J. Geophys. Res. Atmos. 120. http://dx.doi.org/10.1002/2015JD023193.

Li, Z., Xu, Z., Shao, Q., Yang, J., 2009. Parameter estimation and uncertainty analysis of SWAT model in upper reaches of the Heihe river basin. Hydrol. Process. 23 (19), 2744–2753.

Li, X., Cheng, G.D., Liu, S.M., Xiao, Q., Ma, M.G., Jin, R., Che, T., Liu, Q.H., Wang, W.Z., Qi, Y., Wen, J.G., Li, H.Y., Zhu, G.F., Guo, J.W., Ran, Y.H., Wang, S.G., Zhu, Z.L., Zhou, J., Hu, X.L., Xu, Z.W., 2013. Heihe watershed allied telemetry experimental research (HiWATER): scientific objectives and experimental design. Bull. Am. Meteorol. Soc. 94 (8), 1145–1160.

Li, Z.X., Feng, Q., Liu, W., Wang, T.T., Cheng, A.F., Gao, Y., Guo, X.Y., Pan, Y.H., Li, J.G., Guo, R., Jia, B., 2014. Study on the contribution of cryosphere to runoff in the cold alpine basin: a case study of Hulugou River Basin in the Qilian Mountains. Glob. Planet. Chang. 122, 345–361.

Li, Z.X., Feng, Q., Wang, Q.J., Yong, S., Li, H.Y., Li, Y.G., 2016. The influence from the shrinking cryosphere and strengthening evapotranspiration on hydrologic process in a cold basin, Qilian Mountains. Glob. Planet. Chang. 144, 119–128.

Mu, C.C., Zhang, T.J., Wu, Q.B., Peng, X.Q., Cao, B., Zhang, X.K., Cao, B., Cheng, G.D., 2015. Organic carbon pools in permafrost regions on the Qinghai-Xizang (Tibetan) Plateau. Cryosphere 9, 479–496.

Mu, C.C., Zhang, T.J., Zhang, X.K., Cao, B., Peng, X.Q., Cao, L., Su, H., 2016. Pedogenesis and physicochemical parameters influencing soil carbon and nitrogen of alpine meadows in permafrost regions in the northeastern Qinghai-Tibetan Plateau. Catena 141, 85–91.

Niu, L., Ye, B.S., Li, J., Sheng, Y., 2011. Effect of permafrost degradation on hydrological processes in typical basins with various permafrost coverage in western China. Sci. China Ser. D Earth Sci. 41 (1), 85–92.

Osterkamp, T., Romanovsky, V.E., 1997. Freezing of the active layer on the coastal plain of the Alaskan Arctic. Permafr. Periglac. Process. 8, 23–44.

Peterson, B.J., Holmes, R.M., McClelland, J.W., Vörösmarty, C.J., Lammers, R.B., Shiklomanov, A.I., Shiklomanov, I.A., Rahmstorf, S., 2002. Increasing river discharge to the Arctic Ocean. Science 298, 2171–2173.

Piao, S.L., Cui, M.D., Chen, A.P., Wang, X.H., Ciais, P., Liu, J., Tang, Y.H., 2011. Altitude and temperature dependence of change in the spring vegetation green-up date from 1982 to 2006 in the Qinghai-Xizang Plateau. Agric. For. Meteorol. 151 (12), 1599–1608.

Qin, Y., Lei, H.M., Yang, D.W., Gao, B., Wang, Y.H., Cong, Z.T., Fan, W.J., 2016. Long-term change in the depth of seasonally frozen ground an Mountains, northeastern Tibetan Plateau. J. Hydrol. http://dx.doi.org/10.1016/j.jhydrol.2016.09.008.

Romanovsky, V.E., Osterkamp, T., 1997. Thawing of the active layer on the coastal plain of the Alaskan Arctic. Permafr. Periglac. Process. 8 (1), 1–22.

Romanovsky, V.E., Smith, S.L., Christiansen, H.H., 2010. Permafrost thermal state in the polar northern hemisphere during the international polar year 2007–2009: a synthesis. Permafr. Periglac. Process. 21 (2), 106–160.

Saito, K., Kimoto, M., Zhang, T., Takata, K., Emori, S., 2007. Changes in hydro-thermal regimes in frozen ground regions under global warming scenarios simulated by a high-resolution climate model. J. Geophys. Res. 112 (F02S11).

Serreze, M.C., Walsh, J.E., Chapin III, F.S., Osterkamp, T., Dyurgerov, M., Romanovsky, V., Oechel, W.C., Morison, J., Zhang, T., Barry, R.G., 2000. Observational evidence of recent change in the northern high-latitude environment. Clim. Chang. 46, 159–207.

Smith, S.L., Romanovsky, V.E., Lewkowicz, A.G., Burn, C.R., Allard, M., Clow, G.D., Yoshikawa, K., Throop, J., 2010. Thermal state of permafrost in North America–a contribution to the international polar year. Permafr. Periglac. Process. 21, 117–135.

Wang, G.X., Li, Y.S., Wu, Q.B., Wang, Y.B., 2006. Impacts of permafrost changes on alpine ecosystem in Qinghai-Tibet Plateau. Sci. China Ser. D Earth Sci. 49 (11), 1156–1169.

Wang, N.L., Zhang, S.B., He, J.Q., Pu, J.C., Wu, X.B., Jiang, X., 2009a. Tracing the major source area of the mountainous runoff generation of the Heihe River in northwest China using stable isotope technique. Chin. Sci. Bull. 54, 2751–2757.

Wang, G.X., Hu, H.C., Li, T.B., 2009b. The influence of freeze-thaw cycles of active soil layer on surface runoff in a permafrost watershed. J. Hydrol. 375, 438–449.

Wang, G.X., Liu, G.S., Li, C.J., Yang, Y., 2012. The variability of soil thermal and hydrological dynamics with vegetation cover in a permafrost region. Agric. For. Meteorol. 162–163, 44–57.

Wang, Q.F., Zhang, T.J., Wu, J.C., Peng, X.Q., Zhong, X.Y., Mu, C.C., Wang, K., Wu, Q.B., Cheng, G.D., 2013. Investigation on permafrost characteristics over the upper reaches of the Heihe River Basin in Qilian Mountains. J. Glaciol. Geocryol. 35 (1), 19–29 (in Chinese).

Wang, Q.F., Zhang, T.J., Peng, X.Q., Cao, B., Wu, Q.B., 2015a. Changes of soil thermal

regimes in the Heihe River Basin over Western China. Arct. Antarct. Alp. Res. 47, 231–241.
Wang, Y.H., Yang, D.W., Lei, H.M., Yang, H.B., 2015b. Impact of cryosphere hydrological processes on the river runoff in the upper reaches of Heihe River. J. Hydraul. Eng. 46 (9), 1064–1071.
Wang, X.Y., Yi, S.H., Wu, Q.B., Yang, K., Ding, Y.J., 2016a. The role of permafrost and soil water in distribution of alpine grassland and its NDVI dynamics on the Qinghai-Tibetan Plateau. Glob. Planet. Chang. 147, 40–53.
Wang, Q.F., Zhang, T.J., Jin, H.J., Cao, B., Peng, X.Q., Wang, K., Li, L.L., Guo, H., Liu, J., Cao, L., 2016b. Observational study on the active layer freeze–thaw cycle in the upper reaches of the Heihe River of the north-eastern Qinghai-Tibet Plateau. Quat. Int. 440, 13–22. http://dx.doi.org/10.1016/j.quaint.2016.08.027.
Woo, M.K., Kane, D.L., Carey, S.K., Yang, D., 2008. Progress in permafrost hydrology in the new millennium. Permafr. Periglac. Process. 19 (2), 237–254.
Wu, J.C., Sheng, Y., Yu, H., Li, J.P., 2007. Permafrost characteristics in middle east of Qilian Mountains. J. Glaciol. Geocryol. 29 (3), 426–432 (in Chinese).
Wu, Q.B., Hou, Y.D., Yun, H.B., Liu, Y.Z., 2015. Changes in active-layer thickness and near-surface permafrost between 2002 and 2012 in alpine ecosystems, Qinghai-Xizang (Tibet) Plateau, China. Glob. Planet. Chang. 124, 149–155.
Wu, Q.B., Zhang, Z.Q., Gao, S.R., Ma, W., 2016. Thermal impacts of engineering activities and vegetation layer on permafrost in different alpine ecosystems of the Qinghai–Tibet Plateau, China. Cryosphere 10, 1695–1706.
Xu, X.Z., Wang, J.C., Zhang, L.X., 2010. Physics of Frozen Soils. Science Press, Beijing, pp. 130–161 (in Chinese).
Yang, D.Q., Ye, B.S., Kane, D.L., 2004a. Streamflow changes over Siberian Yenisei River basin. J. Hydrol. 296, 59–80.
Yang, D.Q., Ye, B.S., Shiklomanov, A., 2004b. Discharge characteristics and changes over the Ob River watershed in Siberia. J. Hydrometeorol. 5, 595–610.
Yang, Y., Chen, R.S., Ye, B.S., Song, Y.X., Liu, J.F., Han, C.T., Liu, Z.W., 2013. Heat and water transfer processes on the typical underlying surfaces of frozen soil in cold regions (I): water and heat transfer. J. Glaciol. Geocryol. 35 (6), 1545–1554 (in Chinese).
Ye, B.S., Yang, D.Q., Kane, D.L., 2003. Changes in Lena River streamflow hydrology: human impacts versus natural variations. Water Resour. Res. 39, 1200.
Ye, B.S., Yang, D.Q., Zhang, Z.L., Kane, D.L., 2009. Variation of hydrological regime with permafrost coverage over Lena Basin in Siberia. J. Geophys. Res. 114, D07102.
Yi, S.H., Zhou, Z.Y., Ren, S.L., Xu, M., Qin, Y., Chen, S.Y., Ye, B.S., 2011. Effects of permafrost degradation on alpine grassland in a semi-arid basin on the Qinghai-Tibetan Plateau. Environ. Res. Lett. 6 (4), 045103.
Yi, S.H., Wang, X.Y., Qin, Y., Xiang, B., Ding, Y.J., 2014. Responses of alpine grassland on Qinghai-Tibetan plateau to climate warming and permafrost degradation: a modeling perspective. Environ. Res. Lett. 9 (7), 074014.
Zhang, T.J., Frauenfeld, O.W., Serreze, M.C., Etringer, A., Oelke, C., McCreight, J., Barry, R.G., Gilichinsky, D., Yang, D.Q., Ye, H.C., Ling, F., Chudinova, S., 2005. Spatial and temporal variability in active layer thickness over the Russian Arctic drainage basin. J. Geophys. Res. 110, D16101. http://dx.doi.org/10.1029/2004JD005642.
Zhang, X.D., He, J.X., Zhang, J., Polyakov, I., Gerdes, R., Inoue, J., Wu, P.L., 2013a. Enhanced poleward moisture transport and amplified northern high-latitude wetting trend. Nature. Clim. Chang. 3, 47–51.
Zhang, G.L., Zhang, Y.J., Dong, J.W., Xiao, X.M., 2013b. Green-up dates in the Tibetan Plateau have continuously advanced from 1982 to 2011. Proc. Natl. Acad. Sci. U. S. A. 110 (11), 4309–4314.
Zhang, Y.L., Cheng, G.D., Li, X., Han, X.J., Wang, L., Li, H.Y., Chang, X.L., Flerchinger, G., 2013c. Coupling of a simultaneous heat and water model with a distributed hydrological model and evaluation of the combined model in a cold region watershed. Hydrol. Process. 27, 3762–3776.
Zhao, X.Q., Zhou, H.K., 2005. Eco-environmental degradation, vegetation regeneration and sustainable development in the headwaters of the three rivers on the Tibetan Plateau. Bull. Chin. Acad. Sci. 20 (6), 471–476 (in Chinese).
Zhao, L., Cheng, G.D., Li, S.X., Zhao, X.M., Wang, S.L., 2000. Thawing and freezing processes of the active layer in Wudaoliang region of Tibetan Plateau. Chin. Sci. Bull. 45, 2181–2187.
Zhao, L., Wu, Q.B., Marchenko, S.S., Sharkhuu, N., 2010. Thermal state of permafrost and active layer in central Asia during the international polar year. Permafr. Periglac. Process. 21, 198–207.
Zhou, Y.W., Guo, D.X., Qiu, G.Q., Cheng, G.D., Li, S.D., 2000. Frozen Ground in China. Science Press, Beijing, pp. 81–91 (in Chinese).
Zhou, J., Kinzelbach, W., Cheng, G.D., Zhang, W., He, X.B., Ye, B.S., 2013. Monitoring and modeling the influence of snow pack and organic soil on a permafrost active layer, Qinghai-Tibetan Plateau of China. Cold Reg. Sci. Technol. 90 (91), 38–52.
Zhou, J., Pomeroy, J.W., Zhang, W., Cheng, G.D., Wang, G.X., Chen, C., 2014. Simulating cold regions hydrological processes using a modular model in the west of China. J. Hydrol. 509, 13–24.
Zhu, L.N., Wu, Z.W., Zang, E.M., Pan, B.W., Liu, Y.Z., Tao, G.X., 1996. Difference of permafrost degradation in the eastern Tibetan Plateau. J. Glaciol. Geocryol. 18 (2), 104–110 (in Chinese).